



Article

Assessment of the Chemical Reactivity of Brazilian Stone Cutting Plant Waste into Cementitious Matrices

Anderson Batista Passos ¹, Lucas Onghero ², Paulo Ricardo de Matos ³, Tatiane Benvenuti ¹, Laurence Colares Magalhães ⁴, Antonio Pedro Novaes de Oliveira ⁵, José Renato de Castro Pessôa ¹, Lisandro Simão ⁶ and Marcelo Tramontin Souza ^{1,*}

- ¹ Graduate Program in Science, Innovation and Modelling in Materials (PROCIMM), Laboratory of Mechanical Tests and Resistance of Materials (LEMER), State University of Santa Cruz (UESC), Ilhéus 45662-900, BA, Brazil
- ² Graduate Program in Civil Engineering (PPGEC), Laboratory of Nanotechnology Applications in Civil Construction (NANOTEC), Department of Civil Engineering, Federal University of Santa Catarina (UFSC), Florianópolis 88040-900, SC, Brazil
- ³ Academic Coordination, Federal University of Santa Maria (UFSM), Cachoeira do Sul 96503-205, SC, Brazil
- ⁴ Department of Industrial Technology, Federal University of Espírito Santo (UFES), Vitória 29075-910, ES, Brazil
- ⁵ Graduate Program in Materials Science and Engineering (PGMAT), Laboratory of Glass-Ceramic Materials (VITROCER), Federal University of Santa Catarina (UFSC), Florianópolis 88040-900, SC, Brazil
- ⁶ Graduate Program in Materials Science and Engineering (PPGCEM), Research Group VALORA, University of Southernmost Santa Catarina (UNESC), Criciúma 88806-000, SC, Brazil
- * Correspondence: mtsouza@uesc.br



Citation: Passos, A.B.; Onghero, L.; de Matos, P.R.; Benvenuti, T.; Magalhães, L.C.; de Oliveira, A.P.N.; Pessôa, J.R.d.C.; Simão, L.; Souza, M.T. Assessment of the Chemical Reactivity of Brazilian Stone Cutting Plant Waste into Cementitious Matrices. *Sustainability* **2022**, *14*, 16925. <https://doi.org/10.3390/su142416925>

Academic Editors: Harshit Mahandra, Farzaneh Sadri and Monu Malik

Received: 5 November 2022

Accepted: 13 December 2022

Published: 16 December 2022

Publisher's Note: MDPI stays neutral with regard to jurisdictional claims in published maps and institutional affiliations.



Copyright: © 2022 by the authors. Licensee MDPI, Basel, Switzerland. This article is an open access article distributed under the terms and conditions of the Creative Commons Attribution (CC BY) license (<https://creativecommons.org/licenses/by/4.0/>).

Abstract: The problems generated by the ornamental stone extraction and processing industry caused by the inadequate disposal of this waste can negatively affect rivers, lakes, streams, and even natural water reservoirs. This study discusses and evaluates the potentiality and challenges of dimension stone waste (DSW) recycling generated from a Brazilian dimension stone processing industry in Portland cement formulations. Cement pastes with different amounts of DSW (10–30 wt.%), quartz (10 wt.%), and calcium carbonate (10 wt.%) were prepared and characterized in the fresh and hardened states. The results showed that DSW can be used in cement formulations, and its reactivity is governed by the size of the particles. With up to 10% DSW in place of cement, the samples had greater workability and compressive strength at 28 days compared with the reference mix. However, the strength was lower at early ages (3 and 7 days). When DSW is milled, the strength of the samples containing the waste matched the reference values at all ages, and the recommended replacement limit rose to 20%. On the other hand, the particle size reduction significantly decreased the workability. The use of DSW in cement-based formulations is encouraged due to the strong presence of stone processing and cement companies in Brazil and worldwide.

Keywords: dimension stone waste; chemical reactivity; cementitious matrices

1. Introduction

The dimension stone production process comprises five main stages: prospecting, quarrying, transportation, cutting, and finishing [1]. This last stage of the production chain of the stone sector is the activity carried out by marble dealers, which produce polished pieces with pre-defined sizes and thicknesses for use in construction projects or building renovation. Its operations are centered on cutting, gluing, and finishing surfaces and edges of parts. In all the processing stages, water is used to prevent the cutting and polishing discs from overheating and thus reduce dust generation, resulting in a large volume of effluent in sludge form. Tanks and filter presses are sometimes used to remove excess water/moisture and reduce the sludge amount. It is common for factories to hold the

sludge generated in open or closed basins for weeks to allow the water to evaporate and increase the density [2–5].

The problems generated by the ornamental rock extraction and processing industry caused by the improper disposal of these wastes can affect river basins, lakes, and natural water reservoirs, especially when discarded without any previous treatment. DSW has been considered inert. However, some potentially hazardous compounds can be leached with very fine particles [6]. In this sense, ceramics and cement materials are better solutions for encapsulating contaminants from wastes in their structure [6,7].

It is estimated that 70% of the stones get wasted in the mining and processing procedures. In the processing stage, the tailings are fine, coming from sawing blocks and plates and polishing, comprising about 30% of the weight of the stones [8]. It is estimated that in Brazil, more than 5 million tons of coarse waste are generated in quarries, and more than 3 million tons of fines are in the beneficiation process per year [9]. The volume of waste depends on many factors, such as the type of process, size, materials of the cutting and polishing discs, and mineralogy of the stones. Generally, the processing of ornamental rocks generates about 0.1 m^3 of waste per ton of processed stone, with $0.08 \text{ m}^3/\text{t}$ in the sawing process and $0.02 \text{ m}^3/\text{t}$ in the cutting and polishing steps. Both processes produce fine powders with different chemical compositions, depending on the type of stone manufactured [2,6].

In this context, this study evaluated the recycling of dimension stone waste (DSW) in cement matrices. For this, a detailed waste characterization was made, including chemical and physical analyses, and, later, the physicochemical interaction of the waste, as received and comminuted/milled, with the hydrated cement was evaluated. The waste used in this study came from a company located in the city of Itabuna, Bahia, Brazil [6]. This company and others in the region generate large volumes of waste that are often taken to industrial landfills or, in some cases, improperly disposed of. The use of DSW in cementitious materials is encouraged by the massive presence of concrete plants in the study region and throughout Brazil, which could be recipients of these materials.

2. Literature on Dimension Stone Waste Use on Cement Matrices

Although the feasibility of recycling DSW in cement-based matrices has been widely discussed, there are disagreements regarding the optimal content, its influence on the rheological properties of cement mixtures, and the physicochemical interactions between DSW and cement. Detailed in the sequence, the literature survey showed that the ideal SW content relies on its specific surface area, particle size distribution, and chemical composition. The cement-based matrices were also different as some authors replaced DSW with cement and others added it into mortars and concretes. Therefore, this section gathered literature about the effect of DSW in mortars, concretes, and cement pastes.

2.1. DSW Replacing the Fine Aggregates

By using 5 to 15 wt.% DSW with a specific surface area of $11,400 \text{ cm}^2/\text{g}$ as an additive for concretes, Omar et al. [10] observed an increase of ~20% in the compressive strength of concrete after 28 days. As a comparison, typical OPC surface areas usually range from 1500 to $5000 \text{ cm}^2/\text{g}$ [11–15].

Khyaliya et al. [16] replaced part of the sand with DSW in mortar. The authors found that the incorporation of 25 to 50% DSW improved the workability and, consequently, the mechanical performance due to the reduction of the demanded water content (a lower w/c ratio). On the contrary, Şahan Arel et al. [17] noticed reduced workability in replacing DSW with a fine aggregate. Gesoglu et al. [18] replaced up to 20% of the DSW with a concrete binder. The authors observed the need for the addition of superplasticizer to correct the lower workability and slump loss of the concrete, in proportion to the residue content, corroborating the tests conducted by Binici and Yilmaz [19], Hebhoub et al. [20], and Rodrigues et al. [21].

Corinaldesi et al. [22] achieved maximum mechanical strength (~52 MPa) with 10% DSW instead of sand in cement mortar (w/c of 0.5), especially due to the filler effect. For Vardhan et al. [23], the substitution level for the maximum strength and lowest permeability in concrete mixtures with DSW replacing the fine aggregates was 40%.

2.2. DSW Replacing the Cement

Mashaly et al. [24] observed an increase in the mechanical properties of concrete with up to 20% DSW in place of cement while Rana et al. [25] and Vardhan et al. [26] used 10 wt.% Portland cement with DSW. No significant changes were observed in the mechanical performance of the concrete. Vardhan et al. also observed an improvement in workability. Although the authors did not explain why the workability increased, it is reasonable to assume that the reason was the larger particle size of the DSW, the specific surface area of which was significantly smaller ($0.32 \text{ m}^2/\text{g}$) than the residue used by Rana et al. ($0.73 \text{ m}^2/\text{g}$) [25].

Singh et al. [27] demonstrated that DSW can effectively replace up to 15% of the cement, maintaining mechanical properties and improving chloride penetration resistance. Omar et al. [11] examined the filler effect and the chemical interactions' possible contribution to mechanical performance. The authors stated that secondary hydrated calcium silicate can be formed from the reaction of SiO_2 present in DSW with Portlandite in cement. However, this hypothesis has not been confirmed by experimentation. This phenomenon, however, is unlikely, since the SiO_2 of the DSW is mostly crystalline and not very reactive, also evidenced by Musil et al. [28].

Khodabakhshian et al. [29] noted improvements in the mechanical properties of concretes with up to 5 wt.% DSW replacing the cement. These improvements are probably related to the filler effect since the fineness of DSW is considerably higher than that of the aggregates. The authors additionally stated that the formation of carboaluminates can occur due to the reaction between CaCO_3 (present in DSW) and the cement paste. However, little evidence was provided to substantiate these claims.

The filler effect observed by the addition of finer material, such as DSW, in place of fine aggregates is a reasonable consensus in the literature, improving the mechanical strength at the expense of reducing workability (for replacements above ~20%). The reactivity of DSW with cement, however, is still controversial. The insights of this study bring clarity to this point.

3. Materials and Methods

3.1. Raw Materials Characterization

The raw materials used were a high early strength Portland cement (PC) marketed as CP V-ARI (supplied by Supremo Cimento, BR), quartz (purity >98%, density of $\sim 2.7 \text{ g/cm}^3$, Colorminas Colorifício e Mineração Ltd., Içara, Brazil), and calcium carbonate (purity >99%, density of $\sim 2.7 \text{ g/cm}^3$, Lafan Química Fina Ltd., Várzea Paulista, Brazil). The DSW was supplied by a local marble factory in the city of Itabuna, Bahia, Brazil. The quartz and calcium carbonate were also tested in cement pastes to compare with the reactivity of DSW.

The DSW was collected after the ornamental stone cutting stage (see Figure 1). Figure 1a displays the cutting step, where waste generation occurs. Figure 1b shows the channel designed to drain the waste to the storage tanks after cutting (Figure 1c), where the sample was collected (Figure 1d).

The collected sample was dried at 110°C for 24 h and de-agglomerated (named DSW-d) with a planetary mill (Servitech model CT-242/1) without balls for 5 min. The material was then characterized for its particle size distribution using a laser diffraction analyzer (Mastersizer 3000, Malvern Panalytical Ltd., Worcestershire, UK). We also characterized its density with a helium gas pycnometer (Ultrapycnometer1200 P/N, Quantachrome Instruments, Boynton Beach, FL, USA), its surface area (BET, Quantachrome Instruments, NOVA 1200), and X-ray fluorescence spectroscopy (Philips PW 2400, NL) and X-ray diffraction (PANalytical X'Pert PRO, Brighton, UK) were performed with $\text{CuK}\alpha$ radiation, ranging

from $10\text{--}70^\circ 2\theta$ and with a step of $0.5^\circ 2\theta/\text{s}$. Table 1 shows the chemical and mineralogical composition, and the physical characteristics of DSW compared with other ones in the literature.

The waste was also evaluated after milling (named DSW-m) to identify the particle size's influence on the reactivity of cement mixtures. The milling lasted 15 min in an alumina-based planetary ball mill. The target was the comminution to particle sizes of less than $45\ \mu\text{m}$. Subsequently, sieving was performed (mesh #325). The milled waste was again characterized for particle size distribution.

The quartz and calcium carbonate were also characterized in terms of particle size distribution. The Portland cement was characterized with helium gas pycnometry (density), X-ray fluorescence spectroscopy (specific surface area), and X-ray diffraction, complemented by a Rietveld analysis for the quantification of mineralogical phases.

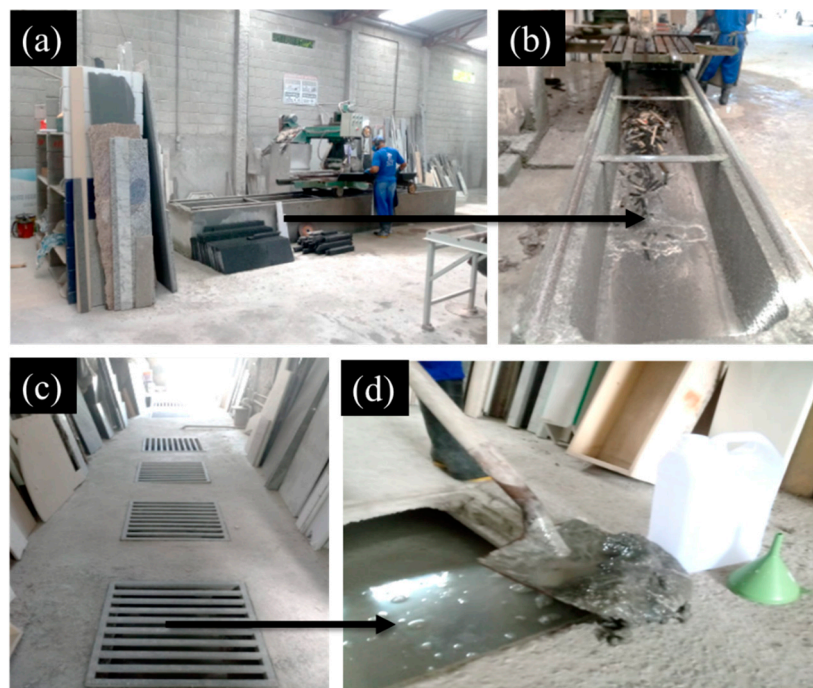


Figure 1. Photographs showing: (a) step of cutting the ornamental rocks, (b) channel designed to drain the generated sludge, (c) storage tanks where the (d) sample was collected.

Table 1. Chemical and mineralogical composition of DSW compared with wastes reported in the literature. Adapted with permission from [6]. LoI: loss on ignition; SSA: specific surface area; ρ : density; Q: quartz; M: muscovite (mica); A: anorthoclase (feldspar); Lime: calcite; Dol: dolomite; Mimicry; Al: albite (feldspar); Bi: biotite (mica); An: anorthite (plagioclase); Or: orthoclase (feldspar); M: microcline (feldspar); K: kaolinite; Pla: plagioclase; Fel: feldspar; I: illite.

References	Chemical and Mineralogical Composition							Physical Features				
	SiO ₂	CaO	Al ₂ O ₃	MgO	Na ₂ O	K ₂ O	Fe ₂ O ₃	LoI	Main Minerals	ρ (g/cm ³)	SSA (m ² /g)	Mean Particle Size (μ m)
This work (DSW)	53.7	13.4	8.9	3.1	2.4	3.5	4.7	9.6	Q; Mu; A; Dol	2.8	2.7	21.2
Simão et al. [6]	2.2–7.0	41.9–50.6	0.6–3.2	1.0–10.3	0.1–0.8	0.2–0.6	0.4–1.7	35.2–44.2	Cal; Dol	2.6	2.5	6.3
Careddu et al. [30]	<0.6	53.2–54.9	<0.3	0.4–0.5	<0.1	<0.1	<0.1	45.1–43.8	Cal	2.7–2.8	1.8–2.4	3.4–5.0
Ercikdi et al. [31]	1.2	55.1	0.5	0.2	<0.1	0.1	0.1	42.7	Cal	2.7	0.3	
Acchar et al. [32]	37.9	19.9	13.6	3.5	3.6	4.3	3.6	12.4	Q; Bi; Al; An; Or; Cal; Dol			
Monteiro et al. [33]	64.1	3.6	13.2	1.6	2.6	4.4	8.2	1.6	Mi; Q; M; Pla			
Viera et al. [34]	67.1	1.9	14.9	0.7	2.9	5.2	4.4	0.5	Fel; Mi; Pla; Q			
Torres et al. [35]	62.1	4.0	12.8	0.8	3.3	4.3	10.6	0.7	Q; Kao; Mi; Al; I; Cal			
Segadães et al. [36]	47.9	12.6	12.6	4.9	2.3	2.3	3.0	13.1	Mi; Q; Al; Cal; Dol			
Vardhan et al. [37]	4.7	28.7	0.2	22.3	0.1	<0.1	0.5	43.7	Cal; Dol			
Khyaliya et al. [16]	3.8	33.1	Trace	17.9			0.1	45.1	Cal; Dol			
Raupp et al. [38]	0.6	54.5	0.1	0.3	<0.1	0.1	0.2	43.0	Cal			
Yavuz et al. [39]	0.0	55.1	0.2	0.2	0.0	<0.1	0.0	43.8	Cal			
Yeşilay et al. [40]	0.5	53.5		1.7	0.1		0.1	44.1	Cal			
Tozsın et al. [41]	50.8	0.8	9.8	0.7	<0.1		0.5	37.2	Dol			

3.2. Cement Pastes: Production and Characterization

Cement pastes with different amounts of DSW-d and DSW-m (10–30 wt.%), quartz (10 wt.%), and calcium carbonate (10 wt.%) were prepared and characterized in the fresh and hardened states (see Table 2). The tests are detailed in the following sections.

Table 2. Formulations tested; w/b = water/binder ratio.

Samples	Cement	w/b	DSW-d	DSW-m	Quartz	Calcium Carbonate
1	95	0.4	5			
2	95	0.4		5		
3	90	0.4	10			
4	90	0.4		10		
5	90	0.4			10	
6	90	0.4				10
7	80	0.4	20			
8	80	0.4		20		
9	70	0.4	30			
10	70	0.4		30		

The influence of the waste (also compared to quartz and calcium carbonate) on the evolution of the yield stress of the cementitious pastes was evaluated utilizing stationary rotational rheometric tests using a HAAKE iQ viscometer with parallel plate geometry (gap of 1 mm). Data were recorded using HAAKETM RheoWin Job Manager software. The test consisted of applying a very low shear rate (in this case, 0.02 s^{-1} —the lowest shear rate allowed by the equipment), while the shear stress was recorded for 180 s [42–46]. The pastes were previously stirred for 3 min at 500 rpm before being cast in the viscosimeter. The test was initiated by applying a pre-shear of 100 s^{-1} for 1 min to equalize the pastes, followed by 1 min of rest. Five measurements were recorded at 5 min intervals for each paste over a limited period of 60 min of analysis.

An isothermal calorimetry test was carried out to investigate the influence of the DSW-d, DSW-m, quartz, and calcium carbonate on the hydration evolution of cement pastes. The samples were mixed at 300 rpm on a mechanical stirrer for 2 min and placed in glass ampoules. These were sequentially sealed and placed in the equipment (TAM Air Isothermal Calorimeter) right after mixing and monitored for 72 h. The heat flow was normalized based on the total mass of the paste.

X-ray diffraction analyses were performed using a MiniFlex II (Rigaku) diffractometer with $\text{CuK}\alpha$ radiation, with a range of $5\text{--}55^\circ 2\theta$ and a step of $0.5^\circ 2\theta/\text{s}$ to characterize the microstructural changes during the hydration process at different hydration times (3, 7, and 28 days). The hydration of the samples was previously interrupted using alcohol for solvent exchange, followed by drying (at room temperature) and defragmentation in an agate mortar until obtaining particles with sizes smaller than $75\text{ }\mu\text{m}$.

The mechanical performance was evaluated by compressive strength tests following the ABNT NBR 5739 Brazilian standard. Five samples of each composition (10 and 20 wt.% DSW-d and DSW-m, respectively, 10 wt.% quartz, and 10 wt.% CaCO_3) were produced. The samples were cast in cylindrical molds (50 mm high \times 20 mm in diameter), sealed, and left in a controlled environment ($23 \pm 3\text{ }^\circ\text{C}$ and $60 \pm 5\%$) until analysis. Between 2–3 h before the compressive strength tests of the samples cured for 3, 7, and 28 days, the samples were removed from the molds and rectified using a precision cutting machine. The compressive strength was carried out in a compression testing machine (Model PC 200CS, manufacturer EMIC) with a load application speed of 5 mm/min. The results were calculated from the average values of five samples for each composition.

4. Results

4.1. Physicochemical Characteristics of the Raw Materials

Figure 2 shows the DSW (a) before and (b) after the drying process and (c) after the de-agglomeration process. As seen, the DSW, as received, showed up in the form of pellets with about 20% moisture. For the material to be used as a raw material in cementitious mixtures, a previous drying and de-agglomeration process is necessary, so the mixing procedure was feasible. The waste was also milled to analyze the influence of the particle size on the reactivity of the material (DSW-m).



Figure 2. Photographs of DSW (a) as-received, (b) dried, and (c) after being de-agglomerated (DSW-d).

Table 3 presents the chemical and physical characterizations of the cement and dimension stone waste (DSW). In the case of the DSW, the compounds SiO_2 and Al_2O_3 were predominant, followed by CaO and MgO .

Table 3. Chemical and physical characterizations of Portland cement (PC) and DSW. LoI = loss on ignition at $950\text{ }^\circ\text{C}$; ρ = real density; SSA = specific surface area.

Chemical Composition (wt.%)												
	CaO	SiO_2	Al_2O_3	MgO	Fe_2O_3	SO_3	K_2O	Na_2O	TiO_2	LoI		
PC	66.1	15.6	4.0	1.6	3.8	3.7	0.6	0.1		3.9		
DSW	8.9	53.7	13.4	3.0	4.7		3.5	2.4	0.9	9.6		
Mineralogical and Physical Characteristics												
	ρ (g/cm^3)	SSA (m^2/g)	D_{10} (μm)	D_{50} (μm)	D_{90} (μm)	C_3S (%)	C_2S (%)	C_3A (%)	C_4AF (%)	Gypsum+ Bassennite (%)	Calcite (%)	Periclase (%)
PC	3.1	5.7				58.3	11.5	2.8	10.0	3.4	8.2	5.0
DSW-d	2.8	2.7	2.5	21.2	82.1							
DSW-m	2.8	4.5	1.3	6.0	30.3							

The low CaO content and small loss on ignition indicated that calcium carbonate was secondary. This was also evidenced by XRD (Figure 3). The main minerals observed were quartz, muscovite ($\text{KAl}_2\text{Si}_3\text{AlO}_{10}(\text{OH})_2$), albite ($\text{NaAlSi}_3\text{O}_8$), and anorthoclase ($\text{Na}_{0.71}\text{K}_{0.29}\text{AlSi}_3\text{O}_8$). The carbonate phase was dolomite ($\text{CaMg}(\text{CO}_3)_2$).

Figure 4 shows the particle size distribution and cumulative frequency of the materials used, with Figure 4a comparing de-agglomerated (DSW-d) and milled (DSW-m) waste, Figure 4b comparing DSW-d with quartz, and Figure 4c comparing DSW-m with calcium carbonate. The percentiles D_{10} , D_{50} , and D_{90} were also indicated. While DSW-d was close to quartz, DSW-m was close to calcium carbonate. Quartz, as an inert material and with a particle size similar to DSW-d, allows determining if DSW-d is reactive (with the “as received” particle size). On the other hand, calcium carbonate tends to be reactive with cement (for very small particle sizes), which can be compared to DSW-m. Thus, DSW-m was processed to match the fineness of calcium carbonate.

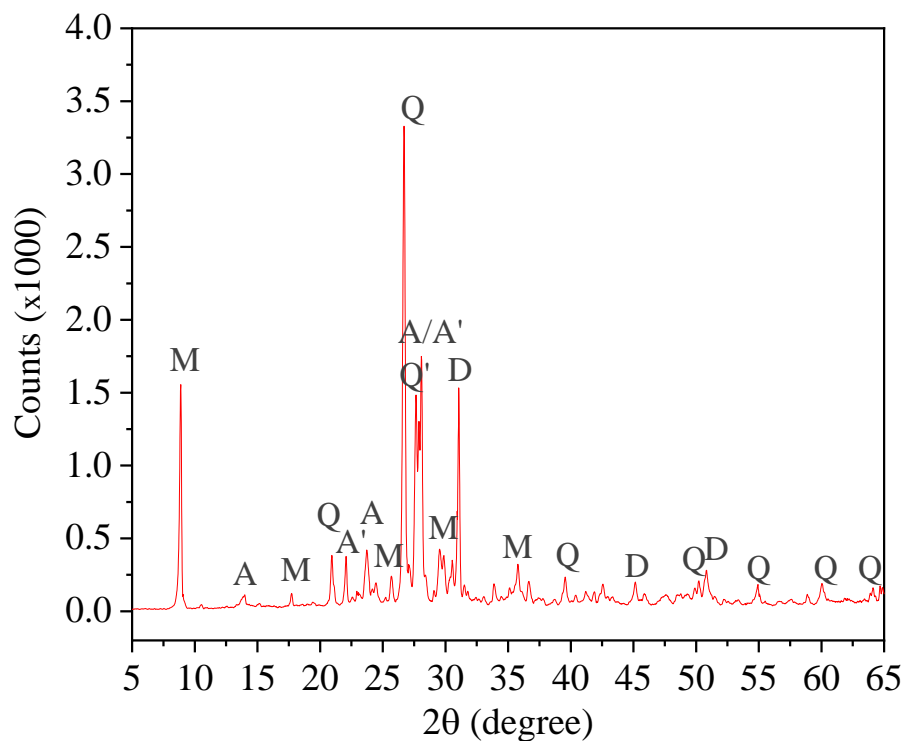


Figure 3. X-ray pattern of DSW. Minerals (cards): Q = quartz (00-046-1045); M = muscovite (00-007-0025); A = anorthoclase (00-010-0361); A' = albite (01-074-0603); D = dolomite (01-071-1662).

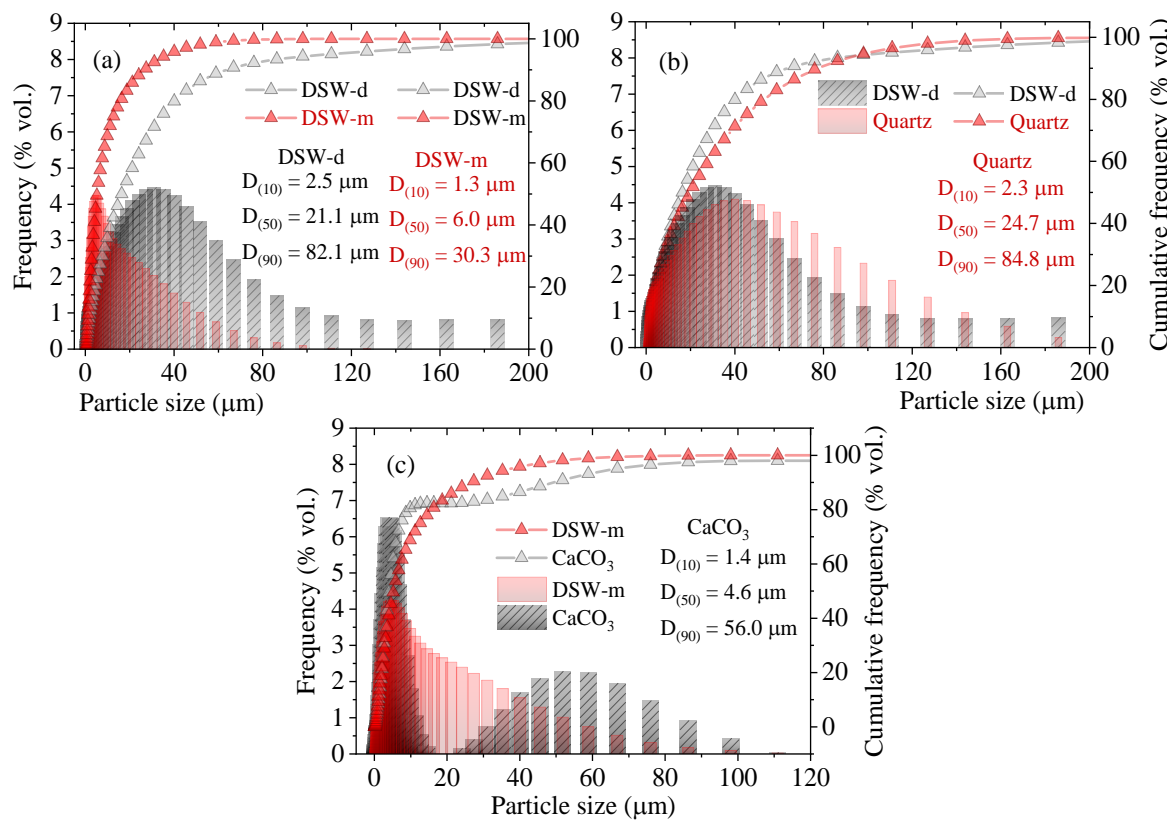


Figure 4. Particle size distribution (PSD) of (a) dry de-agglomerated (DSW-d) and milled (DSW-m) mud, (b) quartz sand, and (c) calcium carbonate.

4.2. Characterization of Cement Pastes

Figure 5 shows the rheological results obtained by rotational rheometry. The replacement of cement with DSW-d at both levels (10 and 20 wt.%) as well as quartz (at 10 wt.%) reduced the yield stress of the pastes for a given testing time compared with the reference sample. This might be associated with the relatively coarser PSD of these materials (D_{50} of 21–25 μm). It is known that the reduction of the particle decreases the interparticle distance, increasing the probability of collision and interparticle friction, consequently increasing the yield stress of the system [47,48]. In contrast, the incorporation of DSW-m and CC increased the yield stress of the pastes, which is explained by the reduced PSD of these particles (D_{50} of around 5–6 μm). Furthermore, it was observed that the structuring rate over time of cement pastes with 10% and 20% DSW-d, as well as for quartz, was slower than that of the Ref, while for 10% DSW-m, the structuring rate was faster, especially from 30 min onward, and was even more intense for calcium carbonate. The structuring rate increase could be associated with the faster formation of hydration products in the samples containing the fine additions (DSW-d and CC)—discussed next based on the calorimetry results—which led to faster water consumption and the quicker formation of a stiff network. On the contrary, the incorporation of coarser particles (DSW-m and CC) in cement replacement resulted in slower water consumption and precipitation rates of hydrated products, reducing the rigidification rate of the material. Finally, it is worth mentioning that the densities of the solid materials were very close, resulting in a negligible difference in the volume of water between the mixtures.

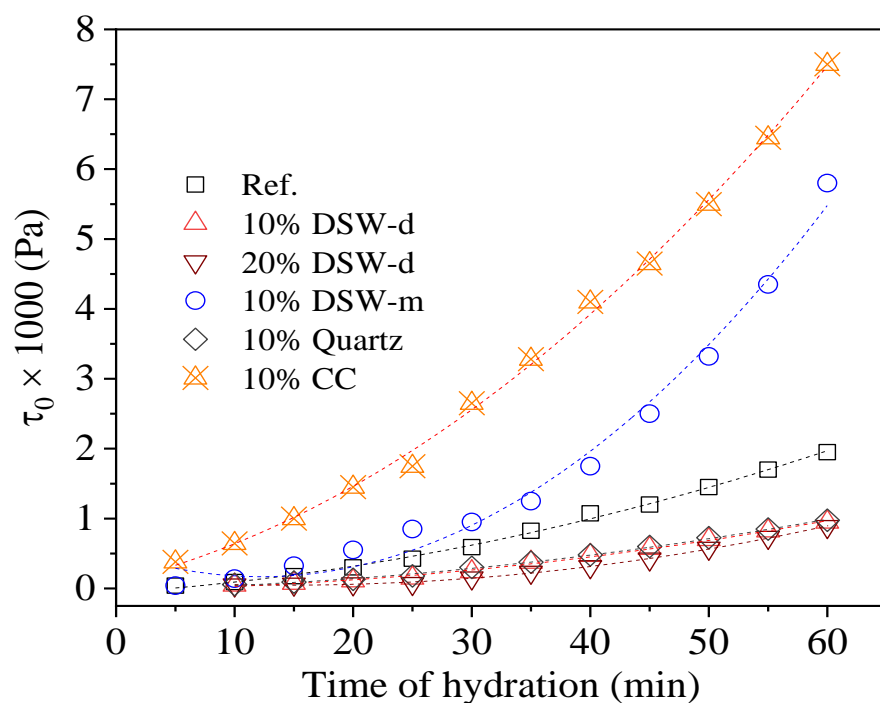


Figure 5. Yield stress (τ_0) obtained with rotational rheometry for cement pastes without and with DSW-d, DSW-m, quartz, and calcium carbonate (CC).

Figure 6 shows the results of isothermal calorimetry results. In Figure 6a, DSW-d is compared to quartz. The heat flow of DSW-d and quartz were less intense than the Ref, especially in the acceleration period, suggesting that both were similarly non-reactive within the first 72 h of hydration. Furthermore, the heat flow was reduced with increasing waste contents (from 10% to 20% DSW-d). In turn, when DSW-m was used (Figure 6b), the heat flow of the sample containing the waste matched the reference sample's value, suggesting that the particle size reduction may favor the interaction (either physical or

chemical) between waste and hydrated cement, as discussed next. For CC, the heat flow was even more intense when compared to the Ref.

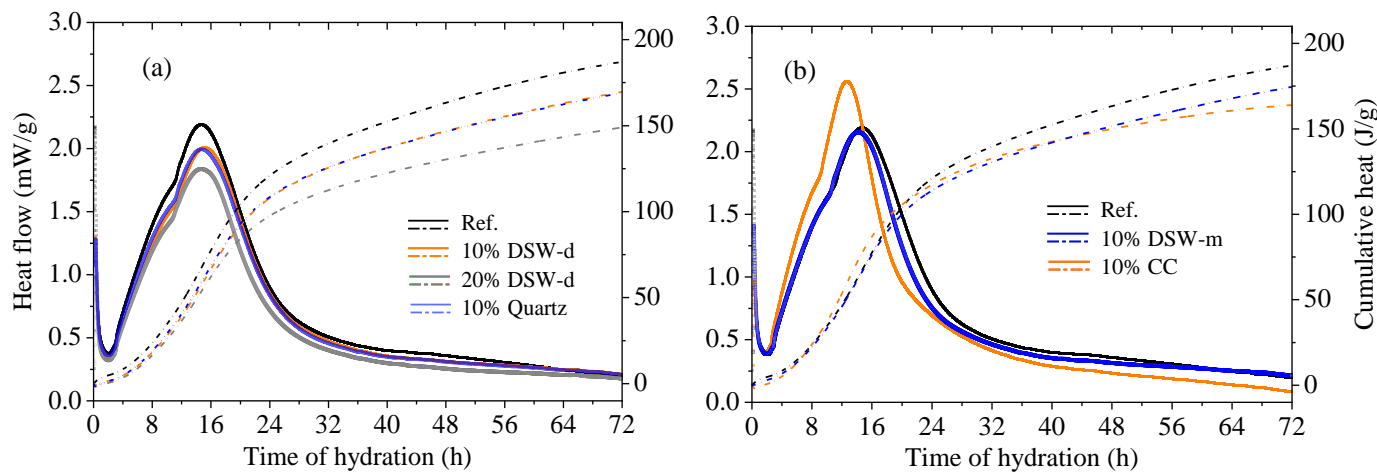


Figure 6. Heat flow (full lines) and cumulative heat (dashed lines) as a function of hydration time of cement pastes with (a) 10% and 20% DSW-d compared with quartz (Q), and (b) DSW-m compared with calcium carbonate (CC).

Calcium carbonate can therefore act as a (non-reactive) filler when coarse or as a reactive addition when fine, accelerating the cement hydration process, widely reported as a nucleating agent [48,49]. Although DSW-m and calcium carbonate have similar particle sizes, the significantly stronger heat flow for calcium carbonate suggests that chemical composition also plays a role. In this sense, it is assumed that DSW from marble processing (with a higher CaCO_3 content) is also capable of accelerating the hydration process if it is fine enough.

Some authors have reported a carboaluminate formation [49–52] from the reaction of CaCO_3 with C_3A and carbosilicate hydrates [53,54] from CaCO_3 and C_3A interactions. In fact, CaCO_3 can accelerate the hydration of C_3S at early ages, and it also acts by producing nucleation sites for the precipitation of calcium silicate hydrates. Ramachandran [50] showed that CaCO_3 accelerated the setting time and strength in C_3S and $\text{C}_3\text{A} + \text{gypsum}$ systems. Ramachandran and Zhang [55] also showed that the acceleration effect in the hydration rate of C_3S was driven by the content and fineness of CaCO_3 .

Moreover, CaCO_3 can interact with C_3A to produce carboaluminates [56–58]. Feldman et al. [59] stated that the addition of CaCO_3 led to the formation of hydrated calcium carboaluminates on the surface of C_3A . Husson et al. [60] observed the presence of calcium silicocarbonates in high levels of CaCO_3 . Vuk et al. [61] observed a reduced setting time with the addition of 5% limestone. Although the compressive strength improved at 2 and 7 days, it worsened at 28 days of hydration.

The presence of carboaluminates can be verified in the X-ray patterns of samples 10% DSW-d, 10% DSW-m, 10% quartz (Q), and 10% CC at 3, 7, and 28 days of hydration (Figure 7). Corroborating the literature [62–64], ettringite remained stable (monosulfate was not detected) at all ages for all samples due to the presence of calcite, including the Ref whose calcite content was estimated at 8.2% (Table 3). The discrete presence of hemicarbonates was also observed. An amplification of the XRD patterns was necessary to be able to detect it since it is a low crystallinity phase and is present at lower levels [65]. The presence of monocarboaluminate was not observed, probably due to the lower availability of alumina.

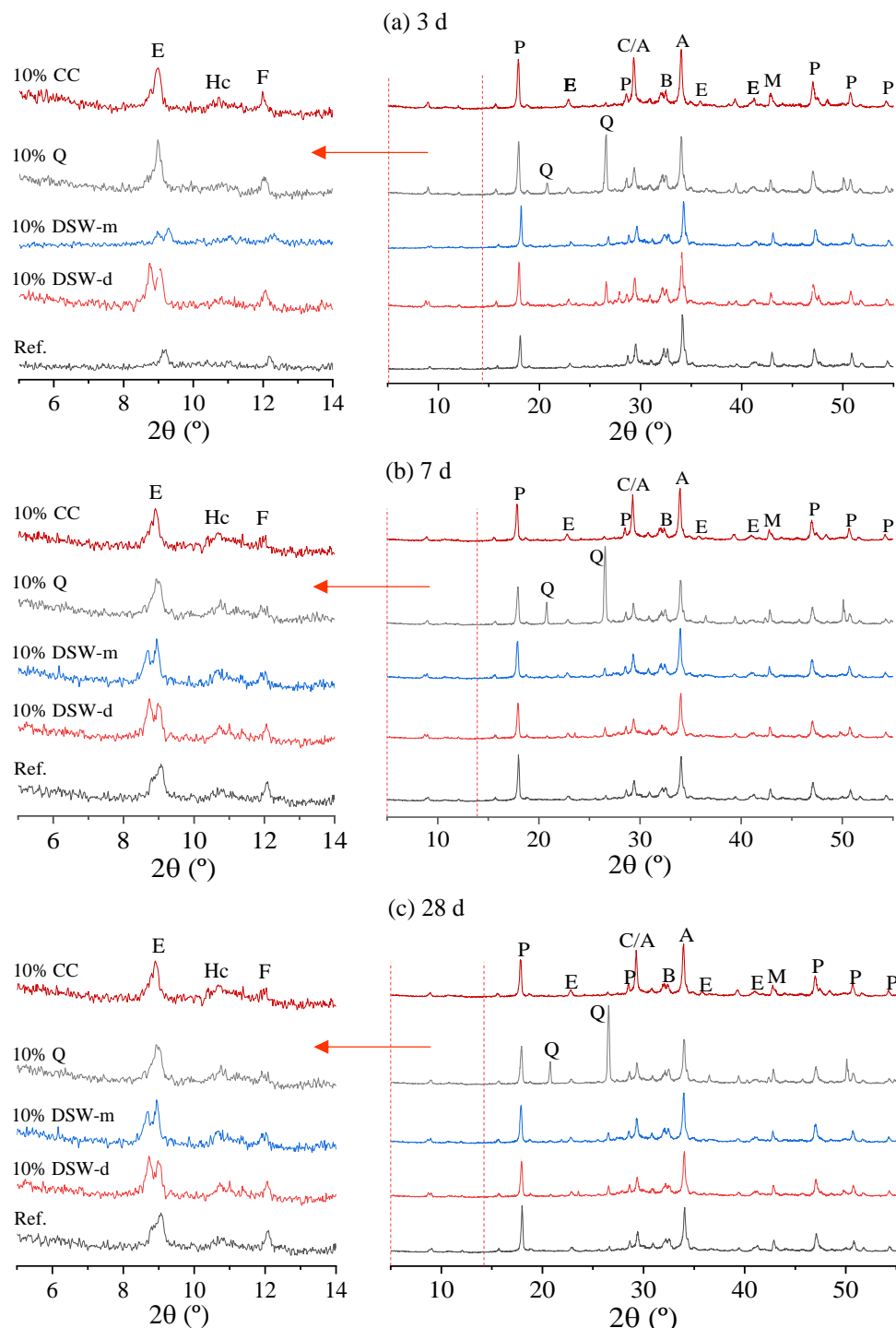


Figure 7. X-ray patterns of samples 10% DSW-d, 10% DSW-m, 10% Q, and 10% CC after (a) 3, (b) 7, and (c) 28 days of hydration. E = ettringite (00-041-1451); P = Portlandite (01-087-0673); A = alite (01-070-8632); B = belite (01-077-0388); M = periclase (00-071-1176); Q = quartz (00-046-1045); C = calcite (00-033-1161); Hc = hemicarboaluminte (41-0221).

Excess calcium carbonate is not reactive with aluminate (C_3A) since the formation of carboaluminates is limited by the availability of alumina. As the content of hemicarbonates did not alter with additional calcium carbonate, it is suggested that the amount of filler in commercial cement is enough to fully react with aluminate. The peak location of calcium carbonate matched with alite at 29.3° . The presence of unreacted calcium carbonate could be verified by observing the 10% CC sample, the peak of which at 29.3° was more intense.

Figure 8a shows the compressive strength results of samples with 10% DSW-d, 10% DSW-m, 10% quartz (Q), and 10% calcium carbonate (CC). With 10% DSW-d and 10% Q, the mechanical strength was significantly reduced, especially at 3 and 7 days. In turn, the 28-day strength values were equivalent. With 10% DSW-m, the strength reduction was less significant, falling within the standard deviations compared to the Ref. The reduction in the waste's particle size, therefore, compensated for the reduction in the cement content, making it more reactive at early ages. The same was observed for CC, except for at 7 days of hydration.

Figure 8b shows the compressive strength at 28 days of hydration of samples with higher levels of DSW-d and DSW-m (up to 30 wt%). It is noted that adding up to 20% DSW-m did not significantly change the strength, neither did it for up to 10% DSW-d. These were, therefore, the maximum levels indicated for cement replacement.

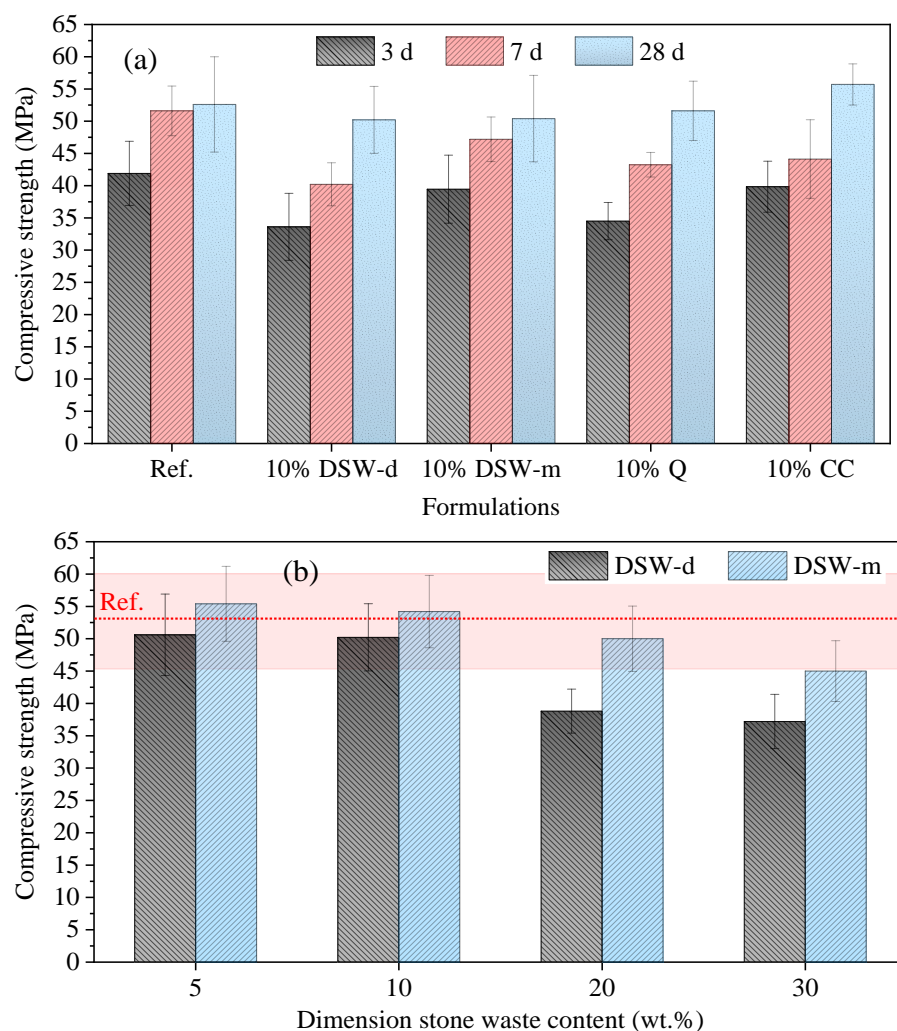


Figure 8. Compressive strength results of samples with (a) 10% DSW-d, 10% DSW-m, 10% Q, and 10% CC after 3, 7, and 28 days of hydration, and with (b) 5% to 30% of DSW-d and DSW-m with 28 days of hydration. The red frame represents the compressive strength of the Ref (mean \pm standard deviation).

5. Conclusions

Despite the literature showing that there is a consensus on the feasibility of recycling DSW for these purposes, there are still many controversies about the ideal content, the effect on the rheological properties of mortars and concretes, and the chemical reactions between DSW and cement.

Through this study, using different characterization techniques, it was possible to identify the physicochemical characteristics of the DSW in the form received and after milling and to evaluate its potential reactivity with the hydrated cement. The results showed that DSW can be used in cementitious matrices, with its reactivity increasing proportionally to the particle size reduction. Using 10 wt.% DSW-m in cement replacement indicated a heat flow evolution similar to the reference sample (containing only Portland cement), also equivalent when comparing the compressive strength. Therefore, the reactivity of stone waste depended on its particle size. In received form, it was practically inert. When milled, its reactivity was higher; however, as there were no apparent microstructural changes in the cementitious paste, it is suggested that DSW acted mainly by increasing the surface area of the solid fraction and acting as a nucleating agent, where the products of hydration precipitate and grow. This is favorable for the reduction of cement consumption and, consequently, for the reduction of cost and environmental impacts; however, the workability of cement-based materials tends to decrease with the increase of substitution.

The introduction of DSW exerted little impact on the content of carboaluminates, the formation of which relied on the aluminate availability. The filler present in commercial cement already did the job. The formation of additional carboaluminates with a DSW addition might be observed, however, in cements with low filler contents (or with more C₃A, although not recommended as a rule).

The insights of this study also bring clarity to the contradictions in the literature related to compressive strength and workability with the use of DSW. The finer the waste, the greater the contribution to strength gain at the expense of reduced workability. When the particle size is small enough, the chemical composition of the DSW becomes an influencing factor. In this case, DSWs with higher contents of carbonaceous phases tended to develop higher strengths at early ages. At 28 days, however, the influence of chemical composition on strength was negligible.

Overall, we can conclude that DSW can be successfully incorporated into cementitious matrices; incorporation levels of up to 20 wt.% of the milled waste or 10 wt.% of the as-received waste did not adversely affect the mechanical performance of the material, leading to similar microstructural characteristics.

Lastly, these findings need to be validated in concrete mixtures, since the presence of aggregates can interfere with the rheological and mechanical properties.

Author Contributions: Conceptualization, M.T.S., L.S. and A.B.P.; methodology, M.T.S., L.S., L.O. and A.B.P.; software, M.T.S. and L.O.; validation, M.T.S., L.O. and L.S.; formal analysis, M.T.S., A.B.P., L.O., L.S. and P.R.d.M.; investigation, M.T.S., L.S., L.O. and A.B.P.; resources, M.T.S., J.R.d.C.P. and A.P.N.d.O.; data curation, M.T.S., L.S. and L.O.; writing—original draft preparation, M.T.S. and L.S.; writing—review and editing, L.O., P.R.d.M., T.B., L.C.M., A.P.N.d.O. and J.R.d.C.P.; visualization, all authors; supervision, M.T.S.; project administration, M.T.S.; funding acquisition, M.T.S. and A.P.N.d.O. All authors have read and agreed to the published version of the manuscript.

Funding: This research was funded by Fundação de Amparo à Pesquisa do Estado da Bahia (FAPESB, project number 073.6766.2020.0010120-57), Coordenação de Aperfeiçoamento de Pessoal de Nível Superior (CAPES)—CAPES-PRINT (project number 88881.310728/2018-01), and Conselho Nacional de Desenvolvimento Científico e Tecnológico (CNPq) (project numbers 402926/2021-8 and 150236/2022-0).

Data Availability Statement: Data will be made available on request.

Conflicts of Interest: The authors declare no conflict of interest.

References

1. Careddu, N.; Dino, G.A. Reuse of Residual Sludge from Stone Processing: Differences and Similarities between Sludge Coming from Carbonate and Silicate Stones—Italian Experiences. *Environ. Earth Sci.* **2016**, *75*, 1075. [[CrossRef](#)]
2. Torres, P.; Fernandes, H.R.; Olhero, S.; Ferreira, J.M.F. Incorporation of Wastes from Granite Rock Cutting and Polishing Industries to Produce Roof Tiles. *J. Eur. Ceram. Soc.* **2009**, *29*, 23–30. [[CrossRef](#)]
3. Ulubeyli, G.C.; Artir, R. Properties of Hardened Concrete Produced by Waste Marble Powder. *Procedia Soc. Behav. Sci.* **2015**, *195*, 2181–2190. [[CrossRef](#)]

4. Demirel, B.; Alyamaç, K.E. Waste Marble Powder/Dust. In *Waste and Supplementary Cementitious Materials in Concrete*; Elsevier: Amsterdam, The Netherlands, 2018; pp. 181–197.
5. Alyamaç, K.E.; Aydin, A.B. Concrete Properties Containing Fine Aggregate Marble Powder. *KSCE J. Civ. Eng.* **2015**, *19*, 2208–2216. [[CrossRef](#)]
6. Simão, L.; Souza, M.T.; Ribeiro, M.J.; Montedo, O.R.K.; Hotza, D.; Novais, R.M.; Raupp-Pereira, F. Assessment of the Recycling Potential of Stone Processing Plant Wastes Based on Physicochemical Features and Market Opportunities. *J. Clean. Prod.* **2021**, *319*, 128678. [[CrossRef](#)]
7. Simão, L.; Hotza, D.; Raupp-Pereira, F.; Labrincha, J.A.; Montedo, O.R.K. Characterization of Pulp and Paper Mill Waste for the Production of Waste-Based Cement. *Rev. Int. Contam. Ambient.* **2019**, *35*, 237–246. [[CrossRef](#)]
8. Akbulut, H.; Gürer, C. Use of Aggregates Produced from Marble Quarry Waste in Asphalt Pavements. *Build. Environ.* **2007**, *42*, 1921–1930. [[CrossRef](#)]
9. Castro, N.F.; Marcon, D.B.; Freire, L.C.; Lima, E.F.; de Almeida, P.F.A. Impacto Do APL de Rochas Ornamentais Do Espírito Santo Nas Comunidades (Impact of the Ornamental Stones APL of Espírito Santo in the Communities). *Cent. Tecnol. Miner. Minist. Ciênc. Tecnol. Inov.* **2012**, *2*, 139–176.
10. Omar, O.M.; Abd Elhameed, G.D.; Sherif, M.A.; Mohamadien, H.A. Influence of Limestone Waste as Partial Replacement Material for Sand and Marble Powder in Concrete Properties. *HBRC J.* **2012**, *8*, 193–203. [[CrossRef](#)]
11. Zunino, F.; Scrivener, K. The Influence of the Filler Effect on the Sulfate Requirement of Blended Cements. *Cem. Concr. Res.* **2019**, *126*, 105918. [[CrossRef](#)]
12. Maier, M.; Sposito, R.; Beuntnner, N.; Thienel, K.-C. Particle Characteristics of Calcined Clays and Limestone and Their Impact on Early Hydration and Sulfate Demand of Blended Cement. *Cem. Concr. Res.* **2022**, *154*, 106736. [[CrossRef](#)]
13. Oey, T.; Kumar, A.; Bullard, J.W.; Neithalath, N.; Sant, G. The Filler Effect: The Influence of Filler Content and Surface Area on Cementitious Reaction Rates. *J. Am. Ceram. Soc.* **2013**, *96*, 1978–1990. [[CrossRef](#)]
14. Mejdi, M.; Saillio, M.; Chaussadent, T.; Divet, L.; Taguit-Hamou, A. Hydration Mechanisms of Sewage Sludge Ashes Used as Cement Replacement. *Cem. Concr. Res.* **2020**, *135*, 106115. [[CrossRef](#)]
15. Bentz, D.P.; Ferraris, C.F.; Galler, M.A.; Hansen, A.S.; Guynn, J.M. Influence of Particle Size Distributions on Yield Stress and Viscosity of Cement–Fly Ash Pastes. *Cem. Concr. Res.* **2012**, *42*, 404–409. [[CrossRef](#)]
16. Khyaliya, R.K.; Kabeer, K.I.S.A.; Vyas, A.K. Evaluation of Strength and Durability of Lean Mortar Mixes Containing Marble Waste. *Constr. Build. Mater.* **2017**, *147*, 598–607. [[CrossRef](#)]
17. Arel, H.S. Recyclability of Waste Marble in Concrete Production. *J. Clean. Prod.* **2016**, *131*, 179–188. [[CrossRef](#)]
18. Gesoğlu, M.; Güneyisi, E.; Kocabağ, M.E.; Bayram, V.; Mermerdaş, K. Fresh and Hardened Characteristics of Self Compacting Concretes Made with Combined Use of Marble Powder, Limestone Filler, and Fly Ash. *Constr. Build. Mater.* **2012**, *37*, 160–170. [[CrossRef](#)]
19. Hanifi, B.; Hasan, K.; Salih, Y. Influence of Marble and Limestone Dusts as Additives on Some Mechanical Properties of Concrete. *Sci. Res. Essays* **2007**, *2*, 372–379.
20. Hebhoub, H.; Aoun, H.; Belachia, M.; Houari, H.; Ghorbel, E. Use of Waste Marble Aggregates in Concrete. *Constr. Build. Mater.* **2011**, *25*, 1167–1171. [[CrossRef](#)]
21. Rodrigues, R.; de Brito, J.; Sardinha, M. Mechanical Properties of Structural Concrete Containing Very Fine Aggregates from Marble Cutting Sludge. *Constr. Build. Mater.* **2015**, *77*, 349–356. [[CrossRef](#)]
22. Corinaldesi, V.; Moriconi, G.; Naik, T.R. Characterization of Marble Powder for Its Use in Mortar and Concrete. *Constr. Build. Mater.* **2010**, *24*, 113–117. [[CrossRef](#)]
23. Vardhan, K.; Siddique, R.; Goyal, S. Strength, Permeation and Micro-Structural Characteristics of Concrete Incorporating Waste Marble. *Constr. Build. Mater.* **2019**, *203*, 45–55. [[CrossRef](#)]
24. Mashaly, A.O.; El-Kalioubi, B.A.; Shalaby, B.N.; El-Gohary, A.M.; Rashwan, M.A. Effects of Marble Sludge Incorporation on the Properties of Cement Composites and Concrete Paving Blocks. *J. Clean. Prod.* **2016**, *112*, 731–741. [[CrossRef](#)]
25. Rana, A.; Kalla, P.; Csetenyi, L.J. Sustainable Use of Marble Slurry in Concrete. *J. Clean. Prod.* **2015**, *94*, 304–311. [[CrossRef](#)]
26. Vardhan, K.; Goyal, S.; Siddique, R.; Singh, M. Mechanical Properties and Microstructural Analysis of Cement Mortar Incorporating Marble Powder as Partial Replacement of Cement. *Constr. Build. Mater.* **2015**, *96*, 615–621. [[CrossRef](#)]
27. Singh, M.; Srivastava, A.; Bhunia, D. An Investigation on Effect of Partial Replacement of Cement by Waste Marble Slurry. *Constr. Build. Mater.* **2017**, *134*, 471–488. [[CrossRef](#)]
28. Musil, L.; Cibulka, T.; Chylik, J.; Vodicka, R. Characterization of Fillers Made of Natural Stones as a Cement Substitute. *IOP Conf. Ser. Mater. Sci. Eng.* **2021**, *1039*, 012007. [[CrossRef](#)]
29. Khodabakhshian, A.; Ghalehnoei, M.; de Brito, J.; Shamsabadi, E.A. Durability Performance of Structural Concrete Containing Silica Fume and Marble Industry Waste Powder. *J. Clean. Prod.* **2018**, *170*, 42–60. [[CrossRef](#)]
30. Careddu, N.; Marras, G.; Siotto, G. Recovery of Sawdust Resulting from Marble Processing Plants for Future Uses in High Value-Added Products. *J. Clean. Prod.* **2014**, *84*, 533–539. [[CrossRef](#)]
31. Ercikdi, B.; Külekci, G.; Yilmaz, T. Utilization of Granulated Marble Wastes and Waste Bricks as Mineral Admixture in Cemented Paste Backfill of Sulphide-Rich Tailings. *Constr. Build. Mater.* **2015**, *93*, 573–583. [[CrossRef](#)]
32. Acchar, W.; Vieira, F.A.; Hotza, D. Effect of Marble and Granite Sludge in Clay Materials. *Mater. Sci. Eng. A* **2006**, *419*, 306–309. [[CrossRef](#)]

33. Monteiro, S.N.; Peçanha, L.A.; Vieira, C.M.F. Reformulation of Roofing Tiles Body with Addition of Granite Waste from Sawing Operations. *J. Eur. Ceram. Soc.* **2004**, *24*, 2349–2356. [[CrossRef](#)]
34. Vieira, C.M.; Soares, T.; Sánchez, R.; Monteiro, S. Incorporation of Granite Waste in Red Ceramics. *Mater. Sci. Eng. A* **2004**, *373*, 115–121. [[CrossRef](#)]
35. Torres, P.; Manjate, R.S.; Quaresma, S.; Fernandes, H.R.; Ferreira, J.M.F. Development of Ceramic Floor Tile Compositions Based on Quartzite and Granite Sludges. *J. Eur. Ceram. Soc.* **2007**, *27*, 4649–4655. [[CrossRef](#)]
36. Segadães, A.M.; Carvalho, M.A.; Acchar, W. Using Marble and Granite Rejects to Enhance the Processing of Clay Products. *Appl. Clay Sci.* **2005**, *30*, 42–52. [[CrossRef](#)]
37. Vardhan, K.; Siddique, R.; Goyal, S. Influence of Marble Waste as Partial Replacement of Fine Aggregates on Strength and Drying Shrinkage of Concrete. *Constr. Build. Mater.* **2019**, *228*, 116730. [[CrossRef](#)]
38. Raupp-Pereira, F.; Ball, R.J.; Rocha, J.; Labrincha, J.A.; Allen, G.C. New Waste Based Clinkers: Belite and Lime Formulations. *Cem. Concr. Res.* **2008**, *38*, 511–521. [[CrossRef](#)]
39. Çelik, M.Y.; Sabah, E. Geological and Technical Characterisation of Iscehisar (Afyon-Turkey) Marble Deposits and the Impact of Marble Waste on Environmental Pollution. *J. Environ. Manag.* **2008**, *87*, 106–116. [[CrossRef](#)]
40. Yeşilay, S.; Çaklı, M.; Ergun, H. Usage of Marble Wastes in Traditional Artistic Stoneware Clay Body. *Ceram. Int.* **2017**, *43*, 8912–8921. [[CrossRef](#)]
41. Tozsin, G.; Oztas, T.; Arol, A.I.; Kalkan, E.; Duyar, O. The Effects of Marble Wastes on Soil Properties and Hazelnut Yield. *J. Clean. Prod.* **2014**, *81*, 146–149. [[CrossRef](#)]
42. Souza, M.T.; Simão, L.; de Moraes, E.G.; Senff, L.; Pessôa, J.R.C.; Ribeiro, M.J.; de Oliveira, A.P.N. Role of Temperature in 3D Printed Geopolymers: Evaluating Rheology and Buildability. *Mater. Lett.* **2021**, *293*, 129680. [[CrossRef](#)]
43. Souza, M.T.; Ferreira, I.M.; Guzi de Moraes, E.; Senff, L.; de Oliveira, A.P.N. 3D Printed Concrete for Large-Scale Buildings: An Overview of Rheology, Printing Parameters, Chemical Admixtures, Reinforcements, and Economic and Environmental Prospects. *J. Build. Eng.* **2020**, *32*, 101833. [[CrossRef](#)]
44. TSouza, M.T.; Ferreira, I.M.; de Moraes, E.G.; Senff, L.; Arcaro, S.; Pessôa, J.R.C.; Ribeiro, M.J.; de Oliveira, A.P.N. Role of Chemical Admixtures on 3D Printed Portland Cement: Assessing Rheology and Buildability. *Constr. Build. Mater.* **2022**, *314*, 125666. [[CrossRef](#)]
45. Souza, M.T.; Sakata, R.D.; Onghero, L.; Magalhães, L.C.; de Campos, C.E.M.; de Oliveira, A.P.N.; Repette, W.L. Insights into the “Accelerating Effect” of Sucrose on Cement Pastes. *J. Build. Eng.* **2022**, *59*, 105053. [[CrossRef](#)]
46. Yuan, Q.; Zhou, D.; Khayat, K.H.; Feys, D.; Shi, C. On the Measurement of Evolution of Structural Build-up of Cement Paste with Time by Static Yield Stress Test vs. Small Amplitude Oscillatory Shear Test. *Cem. Concr. Res.* **2017**, *99*, 183–189. [[CrossRef](#)]
47. Ramos, G.A.; de Matos, P.R.; Pelisser, F.; Gleize, P.J.P. Effect of Porcelain Tile Polishing Residue on Eco-Efficient Geopolymer: Rheological Performance of Pastes and Mortars. *J. Build. Eng.* **2020**, *32*, 101699. [[CrossRef](#)]
48. De Matos, P.R.; de Oliveira, A.L.; Pelisser, F.; Prudêncio, L.R., Jr. Rheological Behavior of Portland Cement Pastes and Self-Compacting Concretes Containing Porcelain Polishing Residue. *Constr. Build. Mater.* **2018**, *175*, 508–518. [[CrossRef](#)]
49. Cochet, G.; Sorrentino, F. Limestone Filled Cements: Properties and Uses. In *Mineral Admixtures in Cement and Concrete*; Sarkar, S.L., Ghosh, S.N., Eds.; ABI Books: New Delhi, India, 1993; pp. 266–295.
50. Ramachandran, V.S. Thermal Analyses of Cement Components Hydrated in the Presence of Calcium Carbonate. *Thermochim. Acta* **1988**, *127*, 385–394. [[CrossRef](#)]
51. Sawicz, Z.; Heng, S.S. Durability of Concrete with Addition of Limestone Powder. *Mag. Concr. Res.* **1996**, *48*, 131–137. [[CrossRef](#)]
52. Tsivilis, S.; Chaniotakis, E.; Badogiannis, E.; Pahoulas, G.; Ilias, A. A Study on the Parameters Affecting the Properties of Portland Limestone Cements. *Cem. Concr. Compos.* **1999**, *21*, 107–116. [[CrossRef](#)]
53. Péra, J.; Husson, S.; Guilhot, B. Influence of Finely Ground Limestone on Cement Hydration. *Cem. Concr. Compos.* **1999**, *21*, 99–105. [[CrossRef](#)]
54. Chloup-Bondant, M.; Edvard, O. Tricalcium Aluminate and Silicate Hydration. Effect of Limestone and Calcium Sulfate. In *NMR Spectroscopy of Cement-Based Materials*; Colombet, P., Grimmer, A.-R., Zanni, H., Sozanni, P., Eds.; Springer: Berlin/Heidelberg, Germany, 1998; p. 295.
55. Ramachandran, V.S.; Zhang, C.M. Influence of CaCO_3 on hydration and microstructural characteristics of tricalcium silicate. *I1 Cem.* **1986**, *3*, 129–152.
56. Trezza, M.; Lavat, A. Analysis of the System $3\text{CaO}\cdot\text{Al}_2\text{O}_3\text{-CaSO}_4\cdot2\text{H}_2\text{O-CaCO}_3\text{-H}_2\text{O}$ by FT-IR Spectroscopy. *Cem. Concr. Res.* **2001**, *31*, 869–872. [[CrossRef](#)]
57. Ramachandra, V.S.; Chun-Mei, Z. Hydration Kinetics and Microstructural Development in the $3\text{CaO}\cdot\text{Al}_2\text{O}_3\text{-CaSO}_4\cdot2\text{H}_2\text{O-CaCO}_3\text{-H}_2\text{O}$ System. *Mater. Struct.* **1986**, *19*, 437–444. [[CrossRef](#)]
58. Kakali, G.; Tsivilis, S.; Aggeli, E.; Bati, M. Hydration Products of C_3A , C_3S and Portland Cement in the Presence of CaCO_3 . *Cem. Concr. Res.* **2000**, *30*, 1073–1077. [[CrossRef](#)]
59. Feldman, R.F.; Ramachandran, V.S.; Sereda, P.J. Influence of CaCO_3 on the Hydration of $3\text{CaO}\cdot\text{Al}_2\text{O}_3$. *J. Am. Ceram. Soc.* **1965**, *48*, 25–30. [[CrossRef](#)]
60. Husson, S.; Guilhot, B.; Pera, J. Influence of Different Fillers on the Hydration of C_3S . In Proceedings of the 9th International Congress on the Chemistry of Cement, New Delhi, India; National Council for Cement and Building Materials (NCB): Odisha, India, 1992.

61. Vuk, T.; Tinta, V.; Gabrovšek, R.; Kaučič, V. The Effects of Limestone Addition, Clinker Type and Fineness on Properties of Portland Cement. *Cem. Concr. Res.* **2001**, *31*, 135–139. [[CrossRef](#)]
62. Lothenbach, B.; Le Saout, G.; Gallucci, E.; Scrivener, K. Influence of Limestone on the Hydration of Portland Cements. *Cem. Concr. Res.* **2008**, *38*, 848–860. [[CrossRef](#)]
63. Matschei, T.; Lothenbach, B.; Glasser, F.P. The Role of Calcium Carbonate in Cement Hydration. *Cem. Concr. Res.* **2007**, *37*, 551–558. [[CrossRef](#)]
64. Zajac, M.; Rossberg, A.; Le Saout, G.; Lothenbach, B. Influence of Limestone and Anhydrite on the Hydration of Portland Cements. *Cem. Concr. Compos.* **2014**, *46*, 99–108. [[CrossRef](#)]
65. Jansen, D.; Naber, C.; Ectors, D.; Lu, Z.; Kong, X.-M.; Goetz-Neunhoeffer, F.; Neubauer, J. The Early Hydration of OPC Investigated by In-Situ XRD, Heat Flow Calorimetry, Pore Water Analysis and ^1H NMR: Learning about Adsorbed Ions from a Complete Mass Balance Approach. *Cem. Concr. Res.* **2018**, *109*, 230–242. [[CrossRef](#)]